Master's Thesis MEE05:20

Real-time Modeling and Analysis of a Multiple-Input-Multiple-Output (MIMO) Wireless System over Acoustic Channel

Farhan Khalid

This thesis is presented as part of the Degree of Master of Science in Electrical Engineering

Blekinge Institute of Technology

April 2005

Master of Science in Electrical Engineering
Blekinge Institute of Technology
Department of Signal Processing
Examiner: Dr. Nedelko Grbic
Supervisor: Dr. Nedelko Grbic

Abstract

Multiple-input-multiple-output (MIMO) wireless systems employ multiple transmitter and receiver antennas, and offer a manifold increase in system capacity and improvement in signal quality, as compared to conventional wireless systems being used at present. MIMO uses spatial multiplexing and exploits multipath propagation to its benefit for increasing system capacity as opposed to conventional wireless systems, while the spatial diversity at the transmitter as well as the receiver ensures better signal quality in terms of the bit-error rate (BER).

This thesis is concerned with the modeling and analysis of a MIMO wireless system using the air acoustic transmission channel. Various performance measures have been carried out on this system in real-time and the results analyzed. The system has been modeled for a stationary indoor environment and demonstrates the application of MIMO principles for data rate maximization.

The designed system is a 2 x 2 MIMO digital transmission system which simultaneously transmits two independent BPSK modulated bit streams. This system makes use of a Singular Value Decomposition (SVD) based MIMO equalization scheme which requires the channel state information (CSI) to be known at the transmitter. Therefore, MIMO channel estimation is also part of the implementation.

The acoustic transmission channel varies considerably from the radio channel. It uses a low carrier frequency and supports very low data rates. In addition, the multipath delay spread may be significantly larger due to slow propagation speed of acoustic waves over large distances. It is comparatively more difficult to model the acoustic channel and multiple filter taps are required for better channel estimation. However, the MIMO principles are equally valid for the acoustic channel as indicated by the results presented in this thesis.

Acknowledgements

I would like to express my gratitude to my supervisor Dr. Nedelko Grbic for his valuable assistance and guidance during the course of this thesis. I would also like to acknowledge the contribution of my teachers at BTH in developing my technical skills which helped me towards successful completion of the thesis work.

Finally, I owe my sincerest regards to my parents who have always been supportive of me in my quest for knowledge.

Farhan Khalid

Table of Contents

List of Figures

Chapter 1

Introduction to MIMO Wireless Systems

1.1 The Need for MIMO

Most wireless communication systems being used at present are Single Input Single Output (SISO) systems where a single transmit (Tx) antenna is used for transmission to a single receive (Rx) antenna. Additional Rx antennas can be used to provide diversity at the receiver. In the days to come, this scenario is likely to change with the advent of Multiple Input Multiple Output (MIMO) communication systems.

MIMO increases system capacity by means of spatial multiplexing, making use of the same frequency resources that would be utilized by a SISO system. As opposed to conventional SISO systems, MIMO systems benefit from multipath propagation and multiply transfer rates by taking advantage of random fading and multipath delay spread [1]. In addition, MIMO provides spatial diversity both at the transmitter and the receiver, thus improving the transmission quality in terms of the bit-error rate (BER).

MIMO equalization schemes usually increases the overall system complexity which can be a matter of concern. However, in recent years the costs of DSP implementation have gone down significantly thus making it possible to create cost effective MIMO systems.

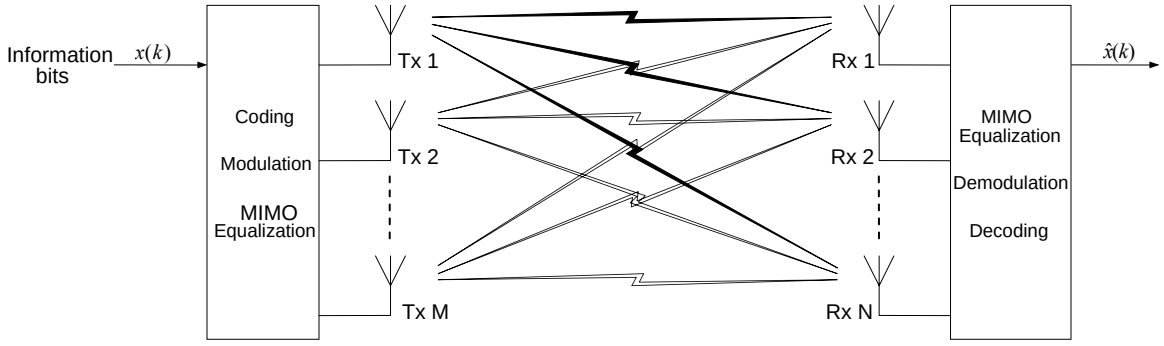

Figure 1.1: *Block diagram of an M x N MIMO wireless system.*

Figure 1.1 shows the general structure of an M x N MIMO wireless system. It can be seen that the MIMO channel is an N x M matrix channel consisting of $M \cdot N$ subchannels. The

MIMO system can also be viewed as a combination of multiple transmit beamformers, each transmitting to one of the *M* Rx antennas.

1.2 MIMO Transmission Schemes

The MIMO transmission schemes can be categorized as data rate maximization schemes or diversity maximization schemes, or a combination of both [1]. Data rate maximization and diversity maximization schemes will be discussed in the following text.

1.2.1 Data Rate Maximization using Spatial Multiplexing

The system capacity i.e. the data rate over MIMO channel can be maximized by means of spatial multiplexing, where independent data streams are transmitted simultaneously over multiple Tx antennas. This can be done for example, by using a *tapped delay line* (TDL) to split a single bit stream into multiple bit streams. These bit streams are spatially decorrelated at the Tx antennas.

The transmitted signals are mixed by the channel. These mixed signals are received at the Rx antennas and require MIMO signal processing at the receiver to unmix them. Richness of the channel in terms of multipath is crucial to the performance of a MIMO system.

An example of spatial multiplexing is the Bell Labs V-BLAST architecture which is discussed in [2].

1.2.2 Diversity Maximization

Diversity maximization schemes are aimed at reducing the BER of the received signal in comparison with SISO systems. This is accomplished by means of the spatial diversity that exists at the transmitter and the receiver of a MIMO system.

Space-time codes (STCs) are used for diversity maximization in MIMO systems. STCs are use to jointly encode multiple Tx antennas to improve BER performance. In space-time coding, the source data stream is encoded in such a way that a number of code symbols equal to the number of Tx antennas are generated and are transmitted simultaneously from each Tx antenna. The structure of the code symbols is such that the decoded signals at the receiver maximize the diversity gain and/or the coding gain [1].

Two main types of STCs exist. These are the *space-time trellis codes* (STTCs) and the *space-time block codes* (STBCs). A discussion and comparison of STTCs and STBCs is provided in [1] and [3].

More recent MIMO techniques like the Geometric Mean Decomposition (GMD) technique proposed in [4] aim at combing the diversity and data rate maximization aspects in an optimal manner.

1.3 MIMO Channel Capacity

The capacity of a memoryless SISO wireless system is given by the Shannon's capacity theorem as [1]

$$C = \log_2(1 + \rho|h|^2) \tag{1.1}$$

where C is the capacity in terms of the spectral efficiency i.e., bits per second per Hz, ρ is the signal to noise ratio (SNR) at the Rx antenna and h is the normalized complex gain of the channel.

If we extend this equation to the case of multiple Rx antennas, the capacity will be given by [1]

$$C = \log_2\left(1 + \rho\sum_{i=1}^{N}|h_i|^2\right) \tag{1.2}$$

where h_i is the gain for the ith Rx antenna, out of the N Rx antennas. Equation (1.2) can also be written as [5]

$$C = \log_2\left[\det\left(\mathbf{I}_N + \rho\mathbf{h}\mathbf{h}^H\right)\right] \tag{1.3}$$

where $\mathbf{I}_N$ is the identity matrix, the vector $\mathbf{h}$ represents the channel gain or transfer function between the single Tx antenna and the Rx antenna array, and $\mathbf{h}^H$ is the Hermitian transpose of $\mathbf{h}$. Equation (1.3) can be extended further to get the capacity of an M x N MIMO system [1]

$$C = \log_2\left[\det\left(\mathbf{I}_N + \frac{\rho}{M}\mathbf{H}\mathbf{H}^H\right)\right] \tag{1.4}$$

where **H** is the N x M MIMO channel matrix. Equation (1.4) assumes that the M information sources are uncorrelated and have equal power. Expressed in terms of eigenvalues, equation (1.4) can be written as [1]

$$C = \sum_{i=1}^{m} \log_2 \left(1 + \frac{\rho}{M} \lambda_i \right) \tag{1.5}$$

where λ_i represent the nonzero eigenvalues of $\mathbf{H}\mathbf{H}^H$ or $\mathbf{H}^H\mathbf{H}$ for $N \leq M$ and $M < N$ respectively and $m = \min(M, N)$.

Equation (1.5) shows that the performance of various MIMO techniques is dependent on the eigenvalue spread i.e. the condition number $\lambda_{max}/\lambda_{min}$. Very low eigenvalues indicate weak transmission channels which may make it difficult to recover the information from the received signals [6]. Therefore, MIMO channel equalization techniques may not work very effectively in scenarios where the eigenvalues are too low or the condition number is too high.

Chapter 2

The Acoustic MIMO System

2.1 M-Audio Delta 1010 Audio System

The primary audio equipment used for the real-time implementation of the acoustic MIMO system consists of the M-Audio Delta 1010 series PCI sound card and the patchbay/router. The Delta sound card simultaneously supports up to eight speakers and eight microphones over the 8 x 8 analog I/O interface. It supports a total of twelve different sampling frequencies ranging from 8 kHz to a maximum of 96 kHz. Different DMA buffer sizes for the input and output signals can also be selected from a list of preset values.

The sound card is connected to the patchbay/router via a 25-pin D-sub host cable. The router contains eight input and eight output ports thus supporting a maximum of eight speakers and eight microphones for simultaneous operation. Technical details about the Delta 1010 audio system can be found in [7]. The Delta 1010 system components are shown in Figure 2.1 [7].

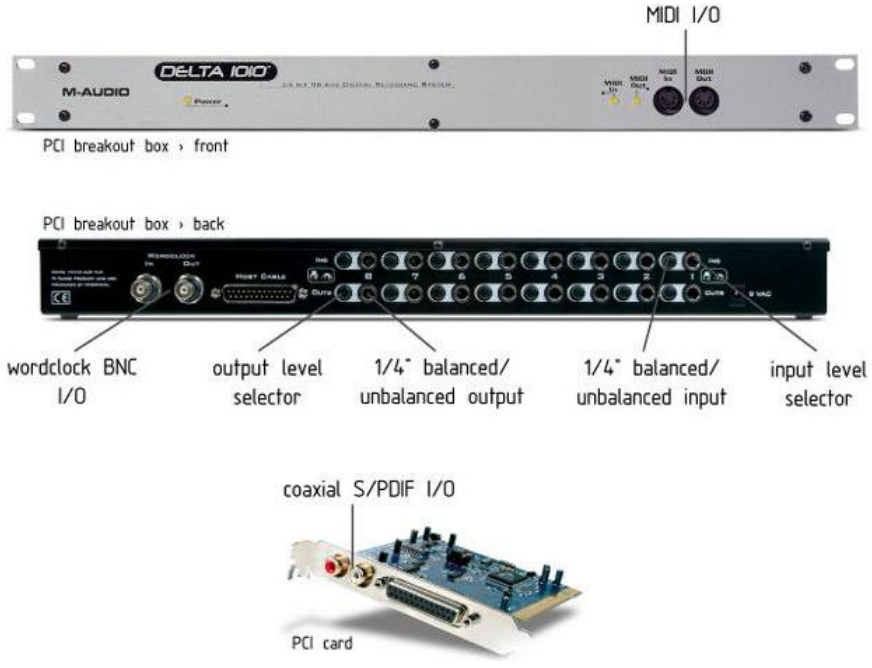

Figure 2.1: *M-Audio Delta 1010 PCI sound card and patchbay/router.*

Figure 2.2 shows the Delta control panel software which allows the selection of sampling rates, DMA buffer sizes and access to several other features and settings.

2.1.1 Delta Control Panel

The Delta Control Panel software provides various configuration settings for the Delta sound card. Figure 2.2 shows the Hardware Settings tab of the Delta Control Panel software which provides options for selecting the codec sampling rate, DMA buffer size, master clock type etc. The settings shown in Figure 2.2 have been used for the real-time MIMO system and are consistent with the sampling rate and DMA buffer size values used in the source code.

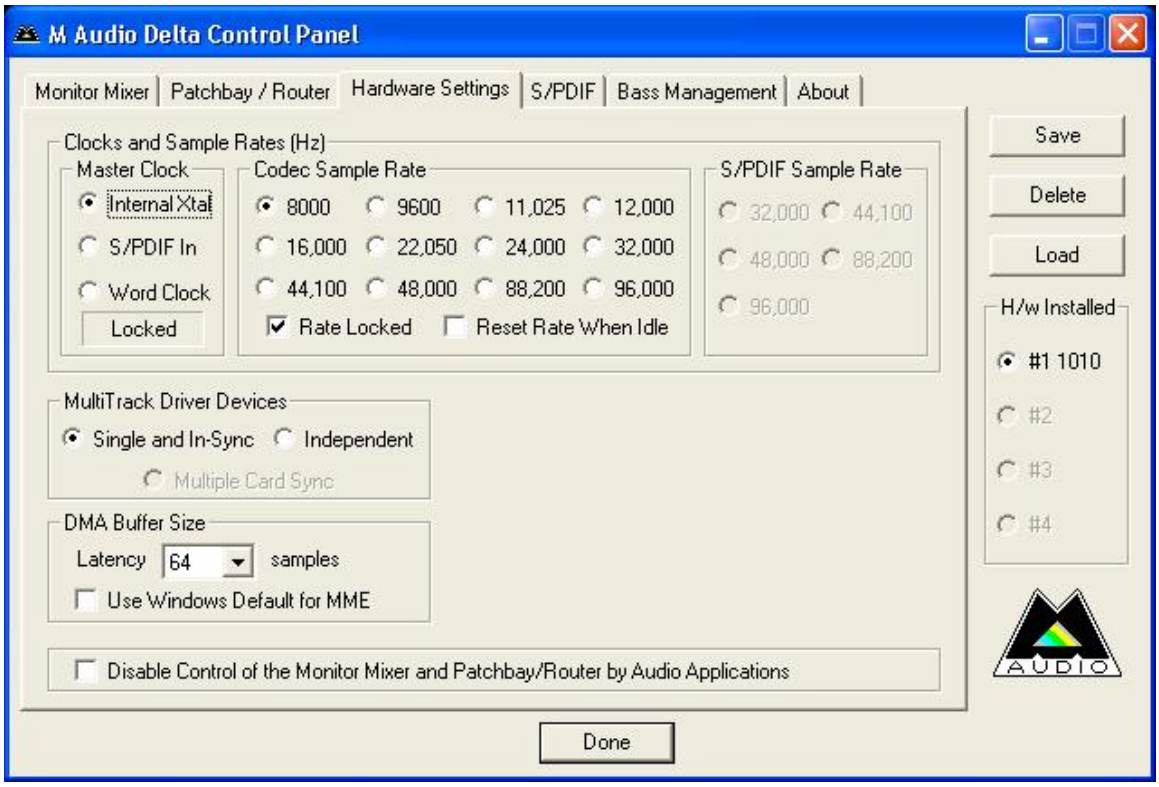

Figure 2.2: *Delta Control Panel Hardware Settings tab.*

2.2 Real-Time Signal Processing Framework

The Real-time Signal Processing (RTSP) Framework [8] is a software tool that provides an interface between the source code written in Matlab and the Delta 1010 sound card drivers for real-time implementation. In other words, the system to be created can be

programmed in Matlab alone and then compiled along with the RTSP framework code to implement the system in real-time using the Delta 1010 audio hardware.

The real-time implementation involves compiling the Matlab m-files data.m and start.m containing the source code, using the Matlab compiler which generates the equivalent C code. This code is compiled and linked along with the RTSP framework files by invoking the Microsoft Visual C++ compiler to generate an executable file. Executing this file makes the real-time system work. Compilation and linking can be performed simply by running a batch file that contains the necessary compiler options.

2.2.1 RTSP Configuration Utility

The RTSP Configuration utility allows the user to choose the number of input and output channels to use depending on the requirements of the real-time system being implemented. It also provides the option to set the runtime duration for the executable file and allows the input and output channel data to be saved as wave files. Enabling these options for saving the input and/or output channels may however degrade the real-time performance of the system [8]. For this reason these two options have not been used for the thesis work. Instead, the saving of input and output data is handled within the Matlab code.

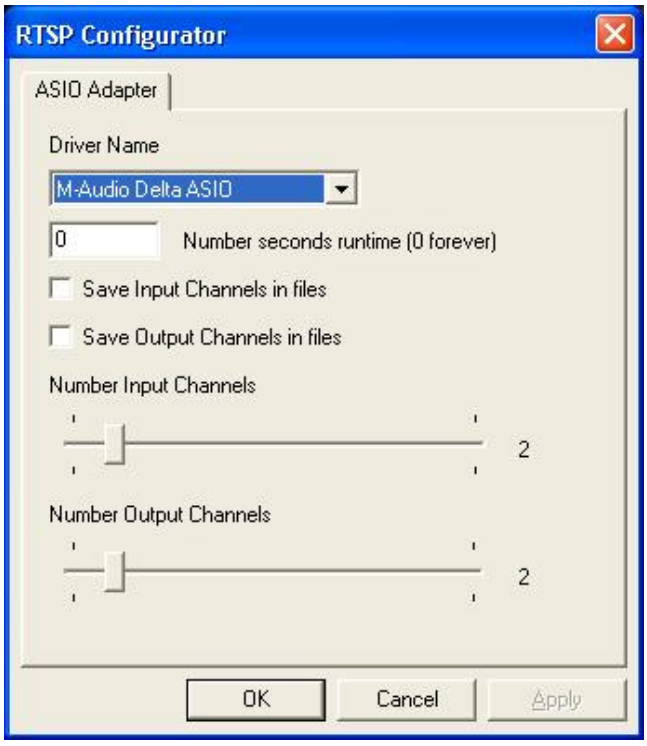

Figure 2.3: *RTSP Configuration utility*.

Figure 2.3 shows a screenshot of the RTSP Configuration utility. The same settings have been used for the 2 x 2 acoustic MIMO system.

2.3 Experimental Setup

The experimental setup for the real-time modeling of the 2 x 2 acoustic MIMO system consists of two non-amplified speakers as transmitters and two microphones as receivers. The speakers are directly connected to the output ports of the Delta 1010 patchbay/router whereas the microphones are connected to the router via pre-amplifiers since the Delta 1010 system does not provide pre-amplification for microphones. The separation between the speaker array and the microphone array is approximately 1.1 meters. The separation between the centers of the speakers is approximately 0.3 meters, same as that between the two microphones.

Figure 2.4: *Experimental setup for the acoustic MIMO system*.

Figure 2.4 shows the experimental setup. The Delta 10101 patchbay/router module can be seen placed directly behind the speakers. The router is connected via a cable to the Delta 1010 PCI sound card installed in a personal computer (PC). The computer is placed outside the soundproof room in order to minimize the noise level within the room. An Intel Pentium 4 processor based PC with Microsoft Windows XP Professional operating system and 768 MB of RAM was used for the experimental setup. The block diagram of the system is shown in Figure 2.5. Individual vector subchannels that constitute the MIMO channel matrix are also shown here.

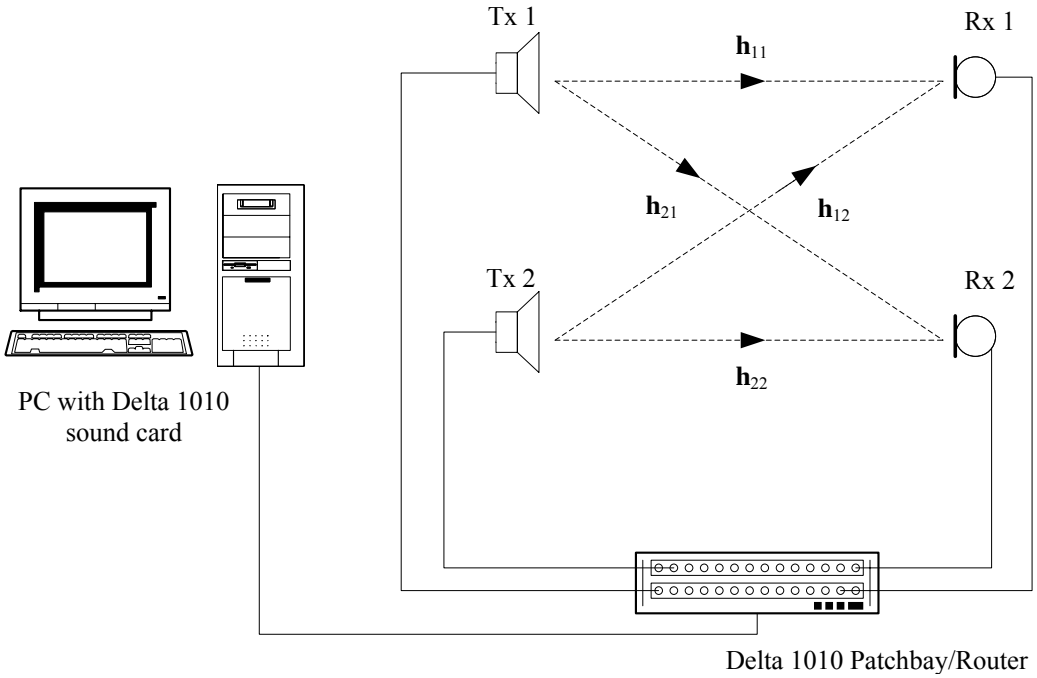

Figure 2.5: *Block diagram of the acoustic MIMO system*.

2.4 Acoustic MIMO System Specifications

The specifications for some important parameters of the implemented acoustic MIMO system are given in Table 2.1.

Parameter	Specification
MIMO configuration	2 x 2
Modulation	BPSK
Carrier Frequency	1 kHz
Sampling Frequency	8 kHz
Data Rate per Tx stream	40 bps
Tx Signal Amplitude (before DAC)	2.14×10^9 (≈ 11 V)
Tx-Rx Seperation	≈ 1.1 m
Tx-Tx & Rx-Rx Seperation	≈ 0.3 m
Tx/Rx DMA buffer size	64 samples

Table 2.1: *Specifications for the acoustic MIMO system*.

BPSK modulation was used because it provides good BER performance on SISO channels with the available audio equipment. High-level modulation techniques are not suitable for the acoustic communication system using the current hardware. The Tx signal amplitude listed in Table 2.1 is the BPSK signal amplitude before digital to analog conversion. The signal levels are internally represented as integer values by the audio device. Increasing the signal amplitude further results in clipping of the signal waveform which introduces additional harmonics in the transmitted signal. Since the speakers were non-amplified, this maximum amplitude level was used to make the transmitted signals audible at the microphones. The DMA buffer size used determines the amount of latency in the received signal apart from the propagation delays. The DMA buffer size setting in Delta Control Panel and the value used in the source code must be the same.

2.5 Operation of the Real-time MIMO System

The real-time acoustic MIMO system simultaneously transmits two binary phase-shift keying (BPSK) modulated independent data streams, which are equalized and transmitted by the speakers as audio signals. These signals are received by the microphones and then equalized and demodulated at the receiver. The implemented MIMO system is aimed at maximizing the transmission data rate.

The real-time system is designed to work in two phases. In the first phase, two short bursts of data (pilot signals) are transmitted simultaneously from each speaker. These data bursts are received by the microphones and then used to estimate the channel at the receiver. MIMO Tx and MIMO Rx filters are then created based on the estimated MIMO channel matrix. The MIMO Rx filter is placed at the receiver before the demodulator while MIMO Tx filter is placed at the transmitter after the modulator. In case of a duplex wireless system, the MIMO Tx filter or the estimated channel matrix could be fed back to

the transmitter using a single transceiver pair. A TDD or FDD system could be used to make the channel state information (CSI) available at the transmitter.

In the second phase, the actual data is transmitted over the MIMO channel with equalization occurring both at the transmitter and the receiver, using the MIMO Tx and MIMO Rx filters respectively. When the transmission has ended, the received data is analyzed and the BER is calculated to evaluate the performance of the MIMO system. Channel estimation and evaluation of MIMO filters may be repeated after a certain duration depending on channel variations in order to ensure good BER performance.

2.6 The Acoustic Environment

The environment for the real-time system can be considered stationary as long as the objects within the room are not moved. However, there might still be some variations since the sound energy from the speakers may excite different objects in different ways. Still, on average, the behavior of the channel remains similar. The noise inside the room has been kept at the minimum possible level by removing any noise sources from the room. However, there are possible internal noise sources within the system, like the microphone preamplifiers.

In order to create a rich scattering environment for the MIMO system, reflecting objects were placed on the outside of the parallel Tx-Rx paths. The line of sight (LOS) between the transmitters and receivers was therefore not blocked completely. This becomes somewhat similar to a Rician fading environment in case of radio channels. The sound waves however, are compressional in nature in contrast to electromagnetic waves. Therefore, it may not be appropriate to apply all of the radio channel characteristics to the acoustic channel. Despite this fact, reflection and scattering mechanisms are similar and therefore allow the creation of rich multipath for implementation of the acoustic MIMO system.

2.7 Applications of Acoustic MIMO Systems

Little work has been done so far in the field of acoustic MIMO systems however certain potential application areas do exist. Acoustic MIMO systems are of particular interest for underwater communications and sonar applications. Underwater acoustic MIMO systems can be used to improve transmission reliability or to increase the communication data rate in comparison with conventional systems.

Another possible application could be the use of ultrasonic MIMO transmission systems in superstores for instantaneously updating the displayed price tags and other product

information for the customers. Use of MIMO would ensure a reliable transmission link in crowded environments. It might also provide a higher throughput, thus opening up the possibility of displaying more detailed product information.

The acoustic MIMO system presented in this thesis can be used as a demonstration system for students to provide an in-depth understanding of the MIMO principles. The transmission system may also serve as a cost-effective solution for testing the performance of different MIMO algorithms using simple modulation techniques.

Chapter 3

MIMO Channel Estimation

3.1 The Acoustic MIMO Channel

The MIMO channel for a 2 x 2 acoustic MIMO system can be represented by the matrix,

$$\mathbf{H} = \begin{bmatrix} \mathbf{h}_{11} & \mathbf{h}_{12} \\ \mathbf{h}_{21} & \mathbf{h}_{22} \end{bmatrix} \tag{3.1}$$

where the vector $\mathbf{h}_{ij}$ represents the channel impulse response between the jth Tx element and the ith Rx element. The 2 x 2 MIMO channel is illustrated in Figure 3.1.

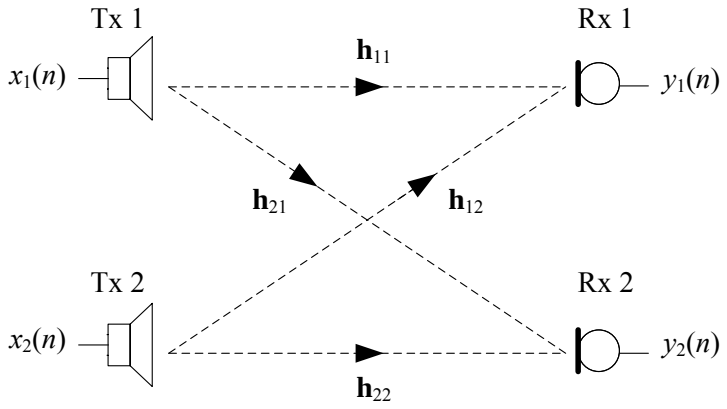

Figure 3.1: *Transmission channel for a 2 x 2 acoustic MIMO system.*

If x_1 and x_2 represent the transmitted signals and y_1 and y_2 are the received signals, then the received signals at time index n may be written as

$$\begin{bmatrix} y_1(n) \\ y_2(n) \end{bmatrix} = \begin{bmatrix} \mathbf{h}_{11} & \mathbf{h}_{12} \\ \mathbf{h}_{21} & \mathbf{h}_{22} \end{bmatrix} \otimes \begin{bmatrix} x_1(n) \\ x_2(n) \end{bmatrix} + \begin{bmatrix} n_1(n) \\ n_2(n) \end{bmatrix} \tag{3.2}$$

or equivalently

$$\mathbf{y} = \mathbf{H} \otimes \mathbf{x} + \mathbf{n} \tag{3.3}$$

where the vector **n** is the additive noise in the received signals and the operator $\otimes$ represents element-wise convolution.

3.2 Prefiltering of Received Signals

Channel estimation for the acoustic MIMO system includes the response of the microphones as well. However, this results in high power DC and low frequency components, which is not desirable. Therefore the received signals have been prefiltered using a highpass equiripple FIR filter. The filter output has been compensated for the group delay. Matlab *filtfilt* function for zero-phase filtering could also be used instead. However, *filtfilt* requires the input sequence to taper to zero at both edges for best results [9]. Filter specifications for the highpass FIR filter are given in Table 3.1.

Parameter	Specification
Stopband edge frequency	50 Hz
Cutoff frequency	550 Hz
Stopband attenuation	40 dB
Filter order	24

Table 3.1: *Specifications for the highpass equiripple FIR filter*.

For the results shown in Figure 4.9, a bandpass equiripple FIR filter was used instead with the specifications given in Table 3.2.

Parameter	Specification
Lower stopband edge frequency	870 Hz
Lower cutoff frequency	930 Hz
Upper cutoff frequency	1.071 kHz
Upper stopband edge frequency	1.131 kHz
Stopband attenuation	60 dB
Filter order	264

Table 3.2: *Specifications for the bandpass equiripple FIR filter*.

The corresponding frequency response of the highpass filter and the bandpass filter is shown in Figure 3.2.

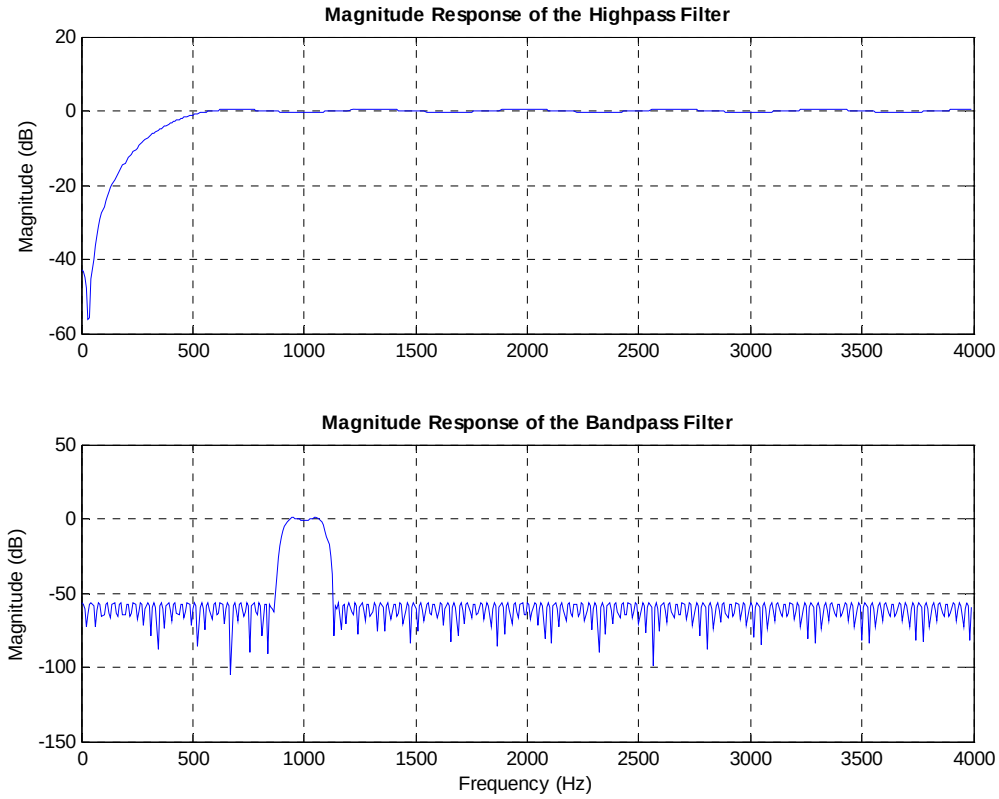

Figure 3.2: *Magnitude response of the highpass filter and the bandpass filter used for prefiltering of the received signals*.

Figure 3.3 shows the power spectral density (PSD) of the signal received by the microphone Rx 1 before and after highpass prefiltering. These results are produced using the channel estimation data before implementing MIMO equalization.

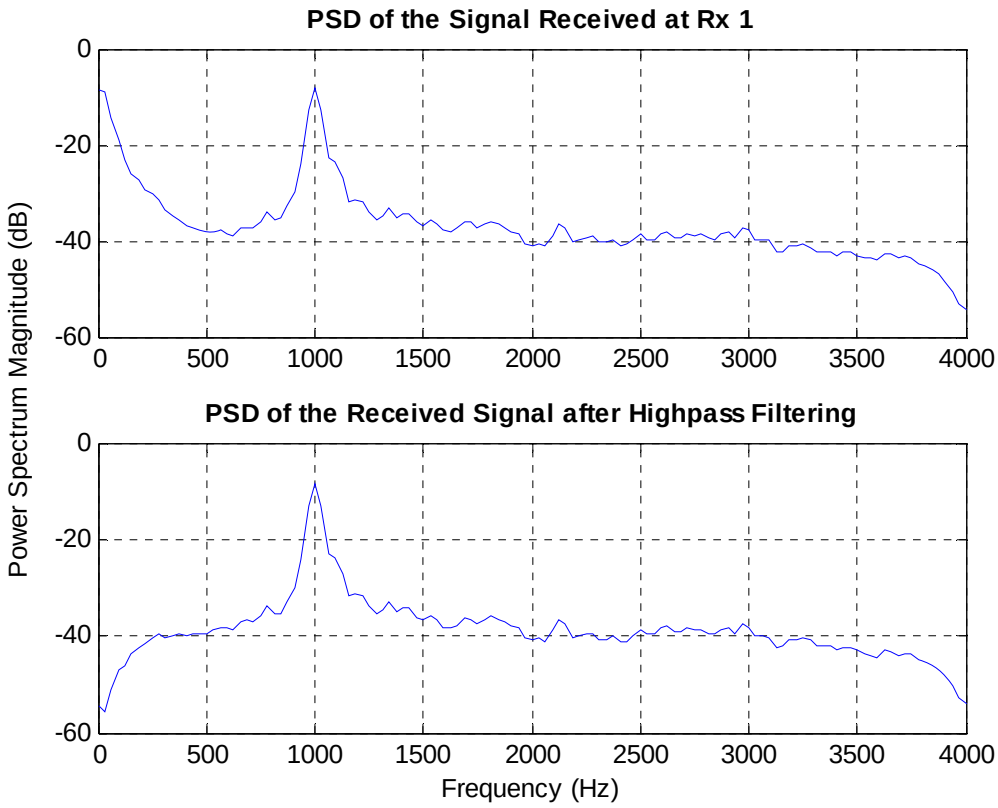

Figure 3.3: *PSD of the received signal at Rx 1 before and after highpass prefiltering.*

3.3 Optimal Least Squares Estimation

The least squares method provides an optimal channel estimate by minimizing the least squares error given by [10]

$$\varepsilon_{LS} = \sum_{n=0}^{N} |e(n)|^2 \tag{3.4}$$

where

$$e(n) = e_{ij}(n) - d_i(n) + y_{ij}(n) = y_{ij}(n) - \hat{y}_{ij}(n) \tag{3.5}$$

is the estimation error at time n for the channel $\mathbf{h}_{ij}$ between Tx j and Rx i, as shown in Figure 3.4. $\hat{y}_{ij}(n)$ represents the corresponding filter output and $d_i(n)$ is the desired signal given by

$$d_i(n) = y_{ii}(n) + y_{ij}(n) \tag{3.6}$$

where $y_{ii}(n)$ is the signal received at Rx i from Tx i and $y_{ij}(n)$ is the signal received at Rx i from Tx j. The desired signals are delay compensated versions of the corresponding Rx signals. The delay compensation is the same for both Rx signals and is equal to the shortest delay in the Rx signals which corresponds to the shortest of the parallel direct paths between the speaker array and the microphone array. The delay includes the latency caused by the DMA buffer and the signal propagation delay from the speakers to the microphones.

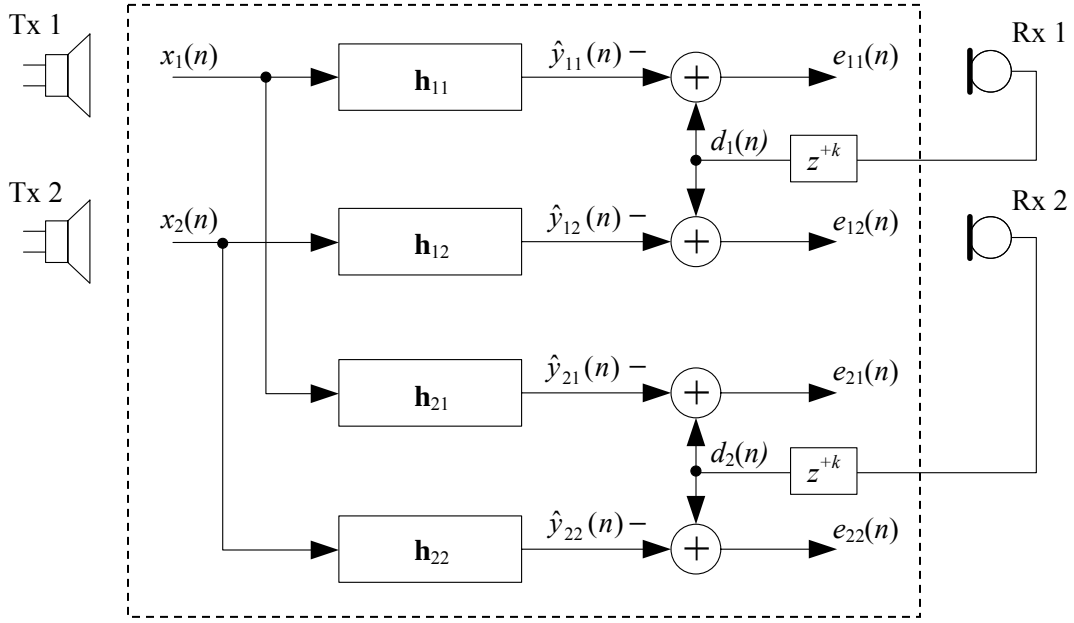

Figure 3.4: *Optimal least squares channel estimation for the 2 x 2 MIMO system.*

The optimal filter coefficients for each of the estimated FIR channel filters shown in Figure 3.4 are given by [10]

$$\mathbf{h}_{ij} = \mathbf{R}_{x_j}^{-1}\mathbf{r}_{d_i x_j} = \mathbf{R}_{x_j}^{+}\mathbf{r}_{d_i x_j} \tag{3.7}$$

where $\mathbf{R}_{x_j}$ is the autocorrelation matrix of the Tx signal $x_j(n)$ and the vector $\mathbf{r}_{d_i x_j}$ represents the cross-correlation between the input signal $x_j(n)$ and the desired signal $d_i(n)$. $\mathbf{R}_{x_j}^{+}$ is the pseudoinverse of the autocorrelation matrix and is equal to the inverse of $\mathbf{R}_{x_j}$ when $\mathbf{R}_{x_j}$ is a full rank square matrix. The autocorrelation matrix is given by

$$\mathbf{R}_{x_j} = \mathbf{X}_j^H \mathbf{X}_j \tag{3.8}$$

where $\mathbf{X}_j$ is a non-symmetric Toeplitz matrix of the form

$$\mathbf{X}_j = \begin{bmatrix} x_j(0) & 0 & 0 & \cdots & 0 \\ \vdots & x_j(0) & 0 & \ldots & 0 \\ x_j(N-1) & \vdots & x_j(0) & \ddots & \vdots \\ 0 & x_j(N-1) & \vdots & \ddots & 0 \\ 0 & 0 & x_j(N-1) & \ddots & x_j(0) \\ \vdots & \vdots & \vdots & \ddots & \vdots \\ 0 & 0 & 0 & \cdots & x_j(N-1) \end{bmatrix} \tag{3.9}$$

where $x_j(n)$; $n = 0, 1, \ldots, N-1$ represent the samples of the input signal of length N. There are $p-1$ zeros in each column where p is the filter length. The autocorrelation matrix is a symmetric Toeplitz matrix with the following structure:

$$\mathbf{R}_x = \begin{bmatrix} r_x(0) & r_x(1) & r_x(2) & \cdots & r_x(p-1) \\ r_x(1) & r_x(0) & r_x(1) & \cdots & r_x(p-2) \\ r_x(2) & r_x(1) & r_x(0) & \cdots & r_x(p-3) \\ \vdots & \vdots & \vdots & \ddots & \vdots \\ r_x(p-1) & r_x(p-2) & r_x(p-3) & \ldots & r_x(0) \end{bmatrix}. \tag{3.10}$$

The cross-correlation vector is given by

$$\mathbf{r}_{dx} = \mathbf{X}^H \mathbf{d}_{N+p-1} \tag{3.11}$$

where the vector $\mathbf{d}_{N+p-1}$ represents the desired signal $d(n)$ for $n = 0, 1, \ldots, N-1$ appended by $p-1$ zeros.

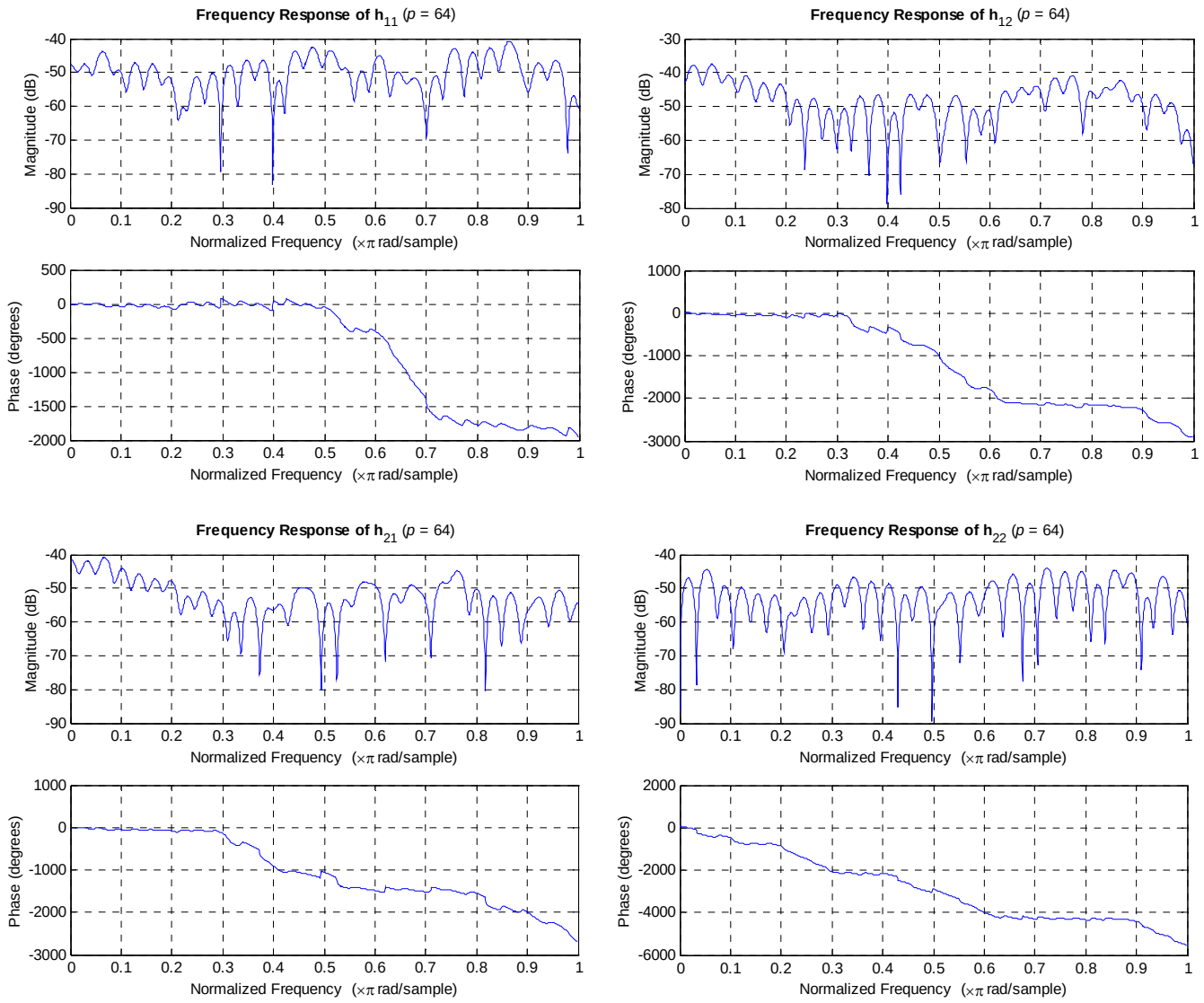

Figure 3.5: *Frequency response of the estimated channel filters with 64 taps.*

Figure 3.5 shows the frequency response of the estimated channels when highpass prefiltering was used. The corresponding impulse response for each of the estimated channel filters is shown in Figure 3.6.

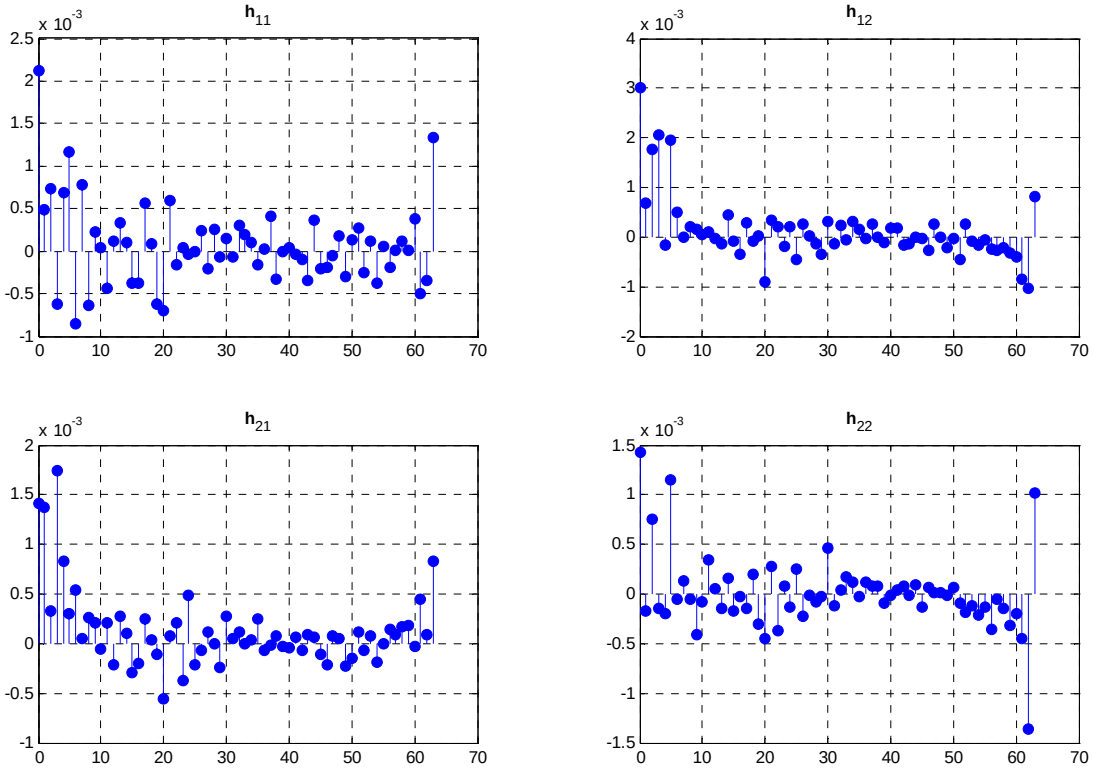

Figure 3.6: *Impulse response of the estimated channel filters*.

Figure 3.7 and Figure 3.8 show the frequency response of the estimated channel filters and the corresponding impulse response when bandpass prefiltering was used.

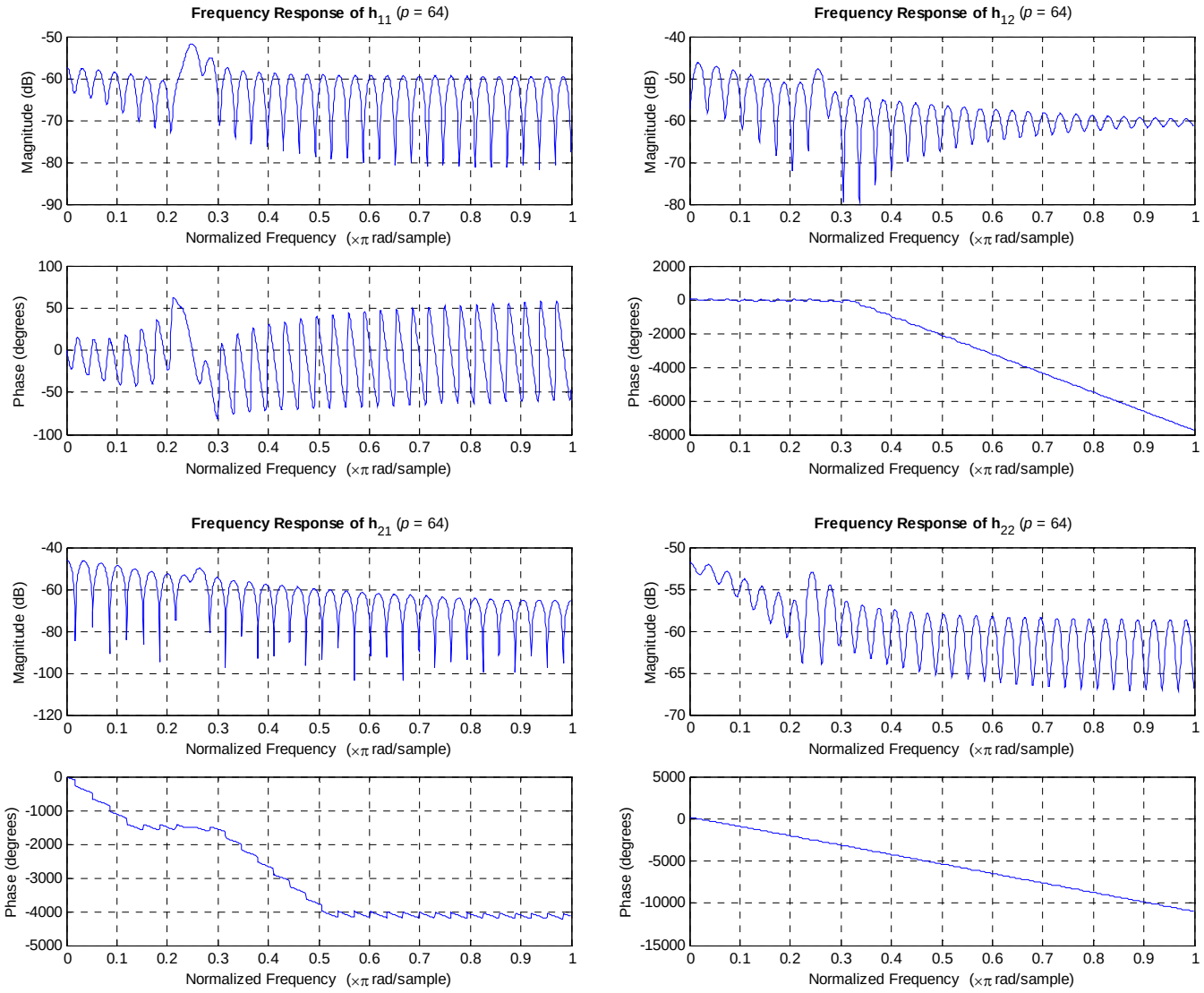

Figure 3.7: *Frequency response of the estimated channel filters with bandpass prefiltering.*

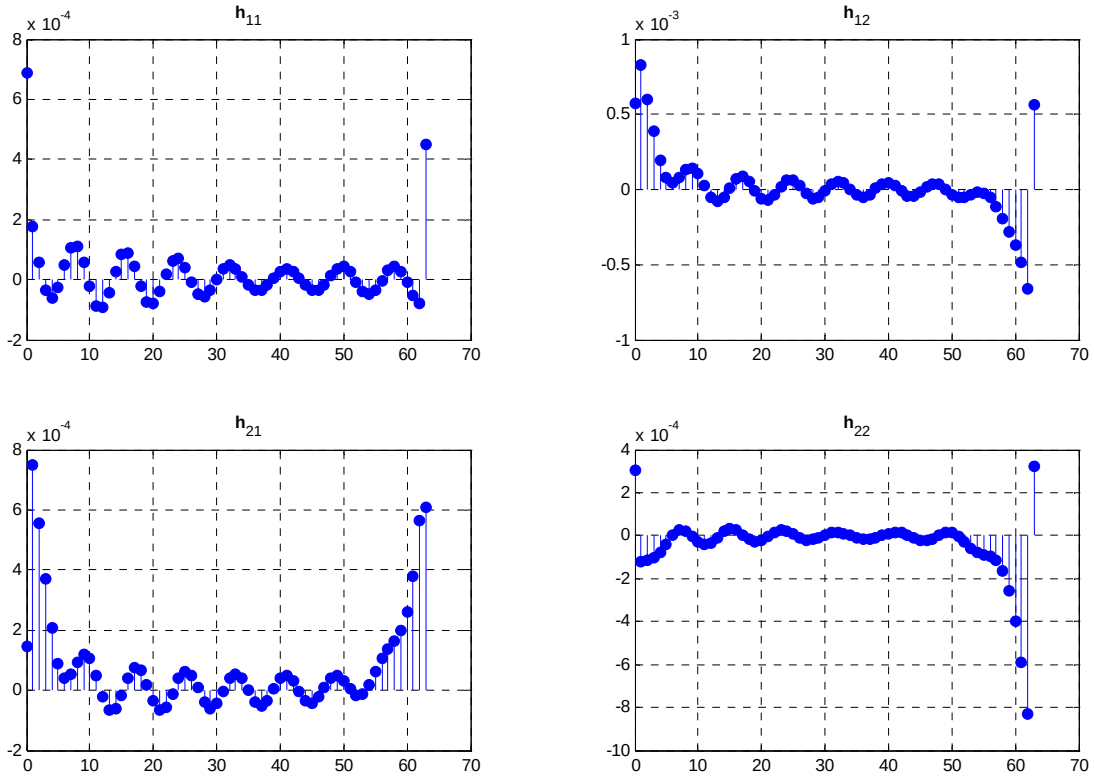

Figure 3.8: *Impulse response of the estimated channel filters with bandpass prefiltering.*

MIMO channel estimation was carried out by simultaneously transmitting 500 bits of data from both speakers, for all of the results presented in this thesis.

3.4 Effect of Channel Condition Numbers

The estimated channels constituting the MIMO channel matrix consist of multiple taps. Therefore Equation (3.1) can be written as

$$\mathbf{H} = \begin{bmatrix} h_{11}(0)\ h_{11}(1) \ldots h_{11}(p-1) & h_{12}(0)\ h_{12}(1) \ldots h_{12}(p-1) \\ h_{21}(0)\ h_{21}(1) \ldots h_{21}(p-1) & h_{22}(0)\ h_{22}(1) \ldots h_{22}(p-1) \end{bmatrix}. \tag{3.12}$$

Taking the discrete Fourier transform (DFT) of each filter in **H**, we have

$$\mathbf{H}_w = \begin{bmatrix} \mathbf{h}_{w11} & \mathbf{h}_{w12} \\ \mathbf{h}_{w21} & \mathbf{h}_{w22} \end{bmatrix} \tag{3.13}$$

which can also be written as

$$\mathbf{H}_w = \begin{bmatrix} h_{w11}(0)\ h_{w11}(1) \ldots h_{w11}(p-1) & h_{w12}(0)\ h_{w12}(1) \ldots h_{w12}(p-1) \\ h_{w21}(0)\ h_{w21}(1) \ldots h_{w21}(p-1) & h_{w22}(0)\ h_{w22}(1) \ldots h_{w22}(p-1) \end{bmatrix}. \quad (3.14)$$

The vector $\mathbf{h}_{w(ij)}$ in Equation (3.13) represents the p-point DFT of the estimated channel filter $\mathbf{h}_{ij}$. The number of points in the DFT has been taken equal to the number of filter taps. The matrix $\mathbf{H}_w$ can be broken down into p subchannel matrices of the form

$$\mathbf{H}_w^{(k)} = \begin{bmatrix} h_{w11}(k) & h_{w12}(k) \\ h_{w21}(k) & h_{w22}(k) \end{bmatrix} \quad ; \quad k \in \{0, 1, \ldots, p-1\} \quad (3.15)$$

where k represents the corresponding DFT bin. Figure 3.9 shows the subchannel matrix condition numbers plotted versus the FFT bins for 64-tap estimated channel filters.

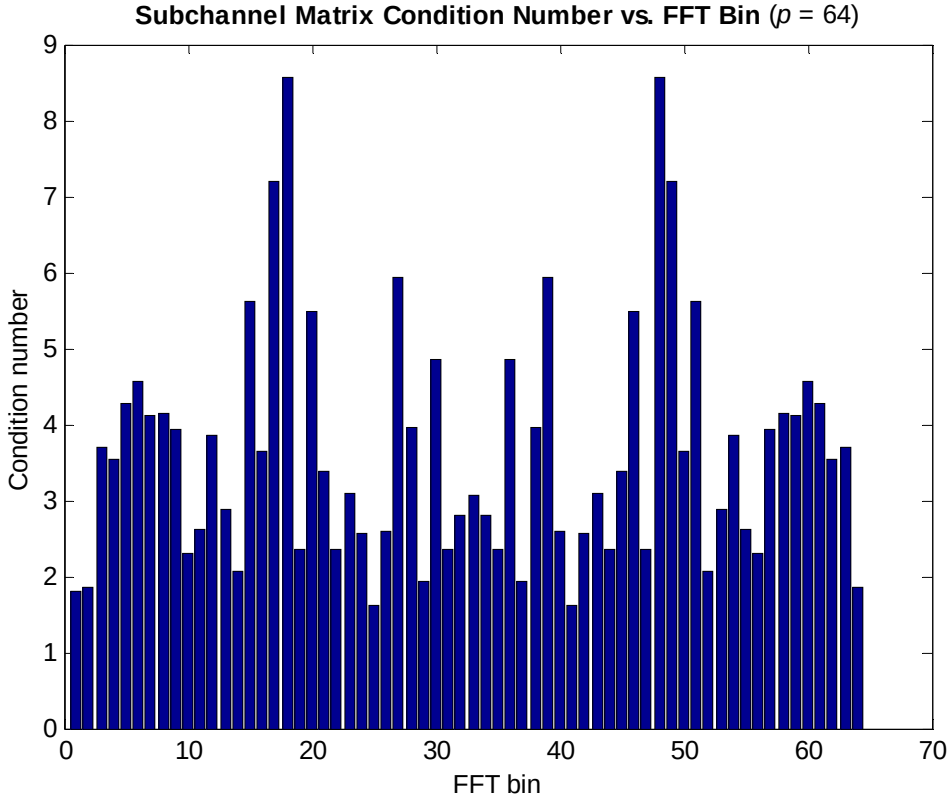

Figure 3.9: *Plot of subchannel matrix condition numbers vs. FFT bins for p = 64.*

The subchannel matrix condition numbers affect the performance of the MIMO system. If the condition numbers for certain FFT bins are too high or if there are several FFT bins with high condition numbers then the system capacity decreases significantly. This is because the channel capacity in MIMO systems is dependent upon the condition number of $\mathbf{HH}^H$ (equals the square of the condition number of $\mathbf{H}$) as given by Equation (1.5)

where **H** is the MIMO channel matrix consisting of scalar channel gains. In case of multiple tap channel filters, the condition number of each subchannel matrix needs to be considered. For this reason, very long filters do not produce good results.

3.5 Channel Fading Characteristics

The acoustic transmission channel for the experimental setup in this thesis is analogous to a Rician fading channel with a very small value of K [11]. The reason for this characterization is that although line of sight (LOS) exists between the Tx and Rx arrays, the multipath components are quite strong and cause heavy fading. The strong echoes come from the reflecting objects placed in close proximity to the setup on either side of the transmission path.

The approximate bandwidth of a BPSK modulated signal is given by [12]

$$B = 2 / T_b = 2R_b \tag{3.16}$$

where T_b is the bit duration and R_b is the bit rate. Using Equation (3.16) it can be seen that most of the Tx signal power lies in the frequency range from 0.24π to 0.26π rad/sample in Figure 3.5. From Figure 3.5 we can see that the magnitude response does not vary much in the frequency range corresponding to the BPSK signal bandwidth and the phase response is approximately constant or linear in that frequency range for all four subchannels. Therefore, each subchannel can be approximated as a flat fading channel. The multipath delay spread of the MIMO channel has been found to be smaller than the BPSK signal bit duration since the distance between the Tx and Rx arrays is short and the data rate is very low, thus confirming the characterization of the acoustic MIMO channel as a flat fading narrowband channel [13]. Increasing the bit rate may however, make the channel frequency selective.

Chapter 4

MIMO Channel Equalization

4.1 SVD based Equalization

The MIMO channel equalization technique used in this thesis is based on singular value decomposition (SVD) of the MIMO channel matrix. Since each vector channel within the acoustic MIMO channel matrix consists of multiple taps, SVD of each subchannel matrix needs to be carried out. The SVD of a 2 x 2 subchannel matrix is given by

$$\mathbf{H}_w^{(k)} = \mathbf{U}_w^{(k)} \mathbf{D}_w^{(k)} \left(\mathbf{V}_w^{(k)}\right)^H \quad ; \quad k \in \{0, 1, \ldots, p-1\} \tag{4.1}$$

where $\mathbf{U}_w^{(k)}$ and $\mathbf{V}_w^{(k)}$ are unitary matrices and $\mathbf{D}_w^{(k)}$ is a diagonal matrix consisting of the singular values of the subchannel matrix along the diagonal. The diagonal matrix can be written as

$$\mathbf{D}_w^{(k)} = \begin{bmatrix} \sigma_1^{(k)} & 0 \\ 0 & \sigma_2^{(k)} \end{bmatrix} = \begin{bmatrix} \sqrt{\lambda_1^{(k)}} & 0 \\ 0 & \sqrt{\lambda_2^{(k)}} \end{bmatrix} \tag{4.2}$$

where $\sigma_i^{(k)}$ represent the singular values and $\lambda_i^{(k)}$ represent the eigenvalues of the subchannel matrix. Each subchannel matrix can be equalized as [14]

$$\left(\mathbf{U}_w^{(k)}\right)^H \mathbf{H}_w^{(k)} \mathbf{V}_w^{(k)} = \left(\mathbf{U}_w^{(k)}\right)^H \mathbf{U}_w^{(k)} \mathbf{D}_w^{(k)} \left(\mathbf{V}_w^{(k)}\right)^H \mathbf{V}_w^{(k)} = \mathbf{D}_w^{(k)}. \tag{4.3}$$

Equation (4.3) implies that the parallel subchannels obtained after equalization corresponding to a particular subchannel matrix will have different gains, equal to the singular values of the subchannel matrix. From the matrices $\mathbf{V}_w^{(k)}$ and $\left(\mathbf{U}_w^{(k)}\right)^H$ we obtain the transfer function of the MIMO Tx and MIMO Rx filter matrices respectively, as given by

$$\mathbf{V}_w = \begin{bmatrix} v_{w11}(0)\ v_{w11}(1) \ldots v_{w11}(p-1) & v_{w12}(0)\ v_{w12}(1) \ldots v_{w12}(p-1) \\ v_{w21}(0)\ v_{w21}(1) \ldots v_{w21}(p-1) & v_{w22}(0)\ v_{w22}(1) \ldots v_{w22}(p-1) \end{bmatrix} \tag{4.4}$$

$$\mathbf{U}_w^H = \begin{bmatrix} u'_{w11}(0) & u'_{w11}(1) \ldots u'_{w11}(p-1) & u'_{w12}(0) & u'_{w12}(1) \ldots u'_{w12}(p-1) \\ u'_{w21}(0) & u'_{w21}(1) \ldots u'_{w21}(p-1) & u'_{w22}(0) & u'_{w22}(1) \ldots u'_{w22}(p-1) \end{bmatrix}. \tag{4.5}$$

In vector notation Equations (4.4) and (4.5) may be written as

$$\mathbf{V}_w = \begin{bmatrix} \mathbf{v}_{w11} & \mathbf{v}_{w12} \\ \mathbf{v}_{w21} & \mathbf{v}_{w22} \end{bmatrix} \tag{4.6}$$

$$\mathbf{U}_w^H = \begin{bmatrix} \mathbf{u}'_{w11} & \mathbf{u}'_{w12} \\ \mathbf{u}'_{w21} & \mathbf{u}'_{w22} \end{bmatrix}. \tag{4.7}$$

The FIR MIMO Tx and Rx filters are obtained by taking the inverse DFT of each vector element in Equations (4.6) and (4.7) respectively.

$$\mathbf{V} = \begin{bmatrix} \mathbf{v}_{11} & \mathbf{v}_{12} \\ \mathbf{v}_{21} & \mathbf{v}_{22} \end{bmatrix} \tag{4.8}$$

$$\mathbf{U}^H = \begin{bmatrix} \mathbf{u}'_{11} & \mathbf{u}'_{12} \\ \mathbf{u}'_{21} & \mathbf{u}'_{22} \end{bmatrix}. \tag{4.9}$$

The matrix $\mathbf{V}$ is the MIMO Tx filter matrix while the matrix $\mathbf{U}^H$ is the MIMO Rx filter matrix, as shown in Figure 4.1.

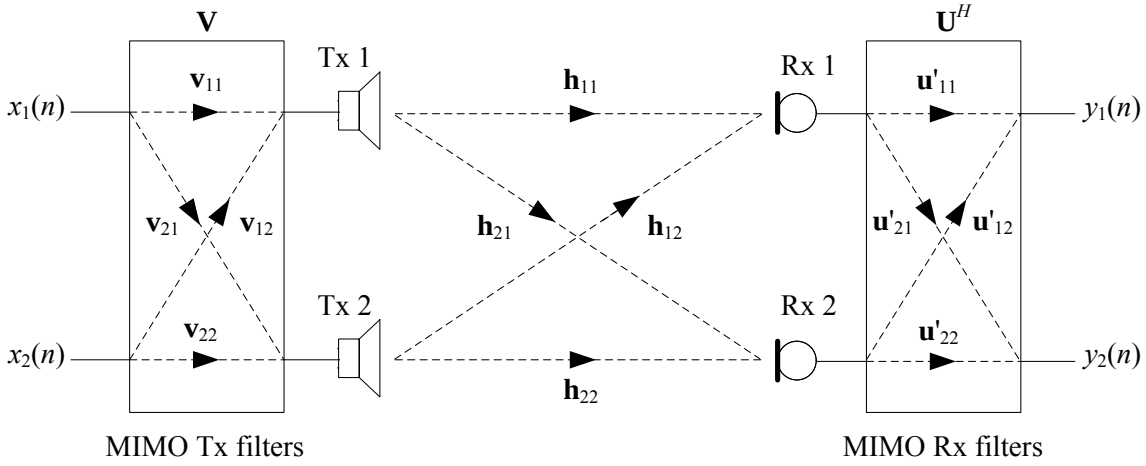

Figure 4.1: *MIMO Tx and Rx filters in the 2 x 2 acoustic MIMO system.*

The equalized signals at the receiver $y_1(n)$ and $y_2(n)$ are the desired signal components retrieved from the mixture. The signal power in different frequency bins for these signals would be different as compared to the mixed signals because of MIMO filtering.

Figures 4.2 to 4.5 show the frequency response and the corresponding impulse response of the MIMO Tx and Rx filters obtained using the estimated MIMO channel given in Figure 3.6.

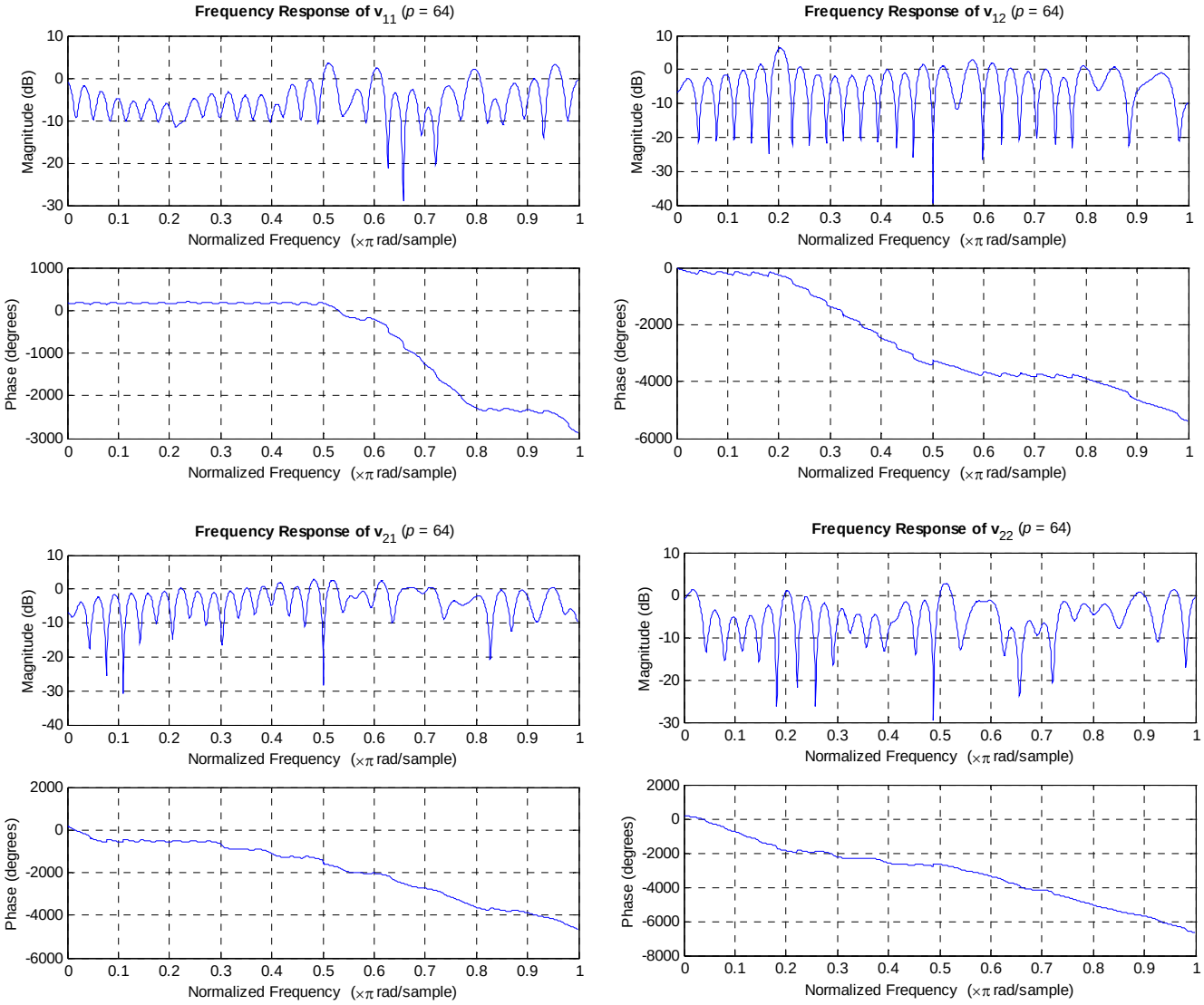

Figure 4.2: *Frequency response of the MIMO Tx filters with 64 taps.*

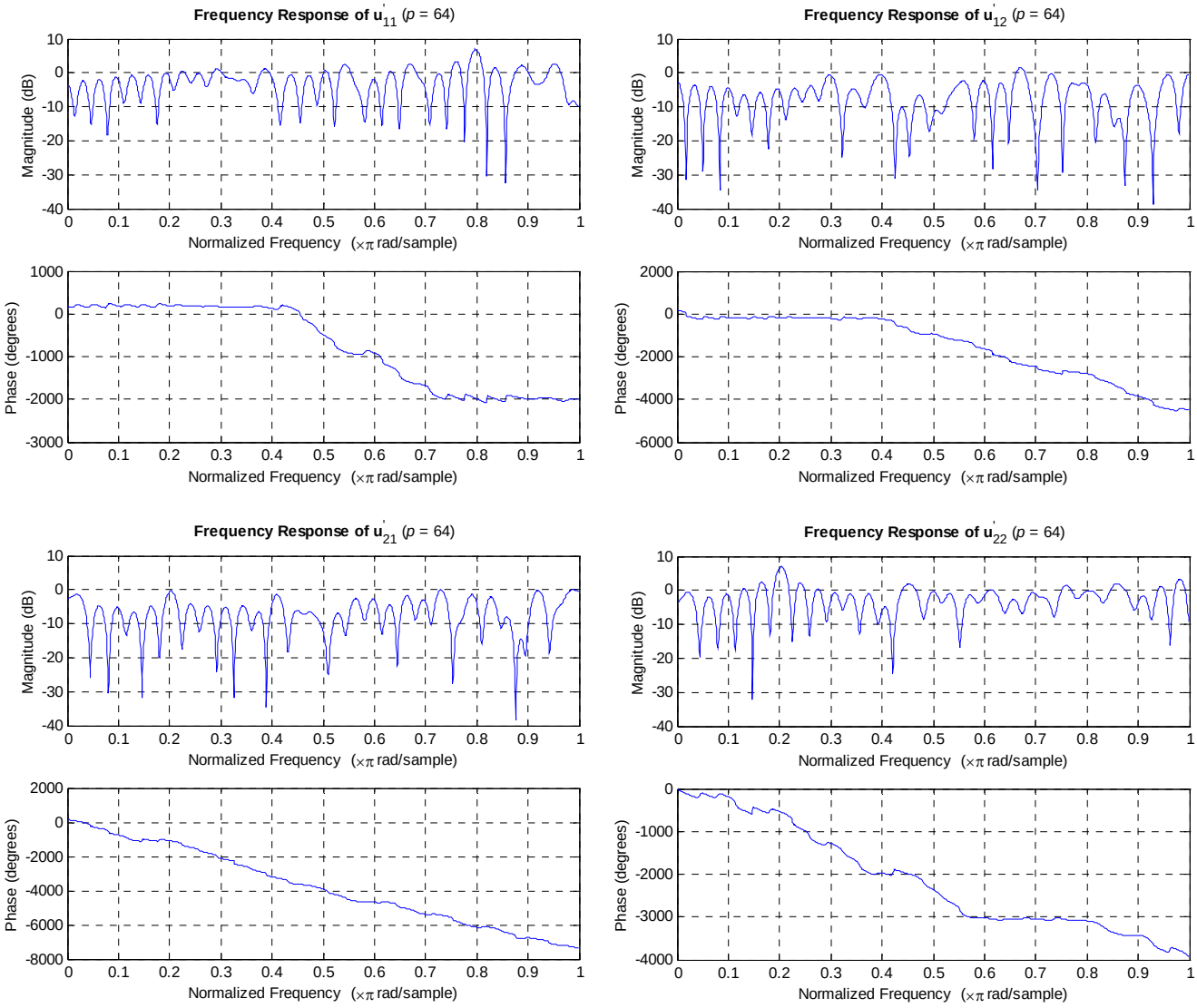

Figure 4.3: *Frequency response of the MIMO Rx filters with 64 taps.*

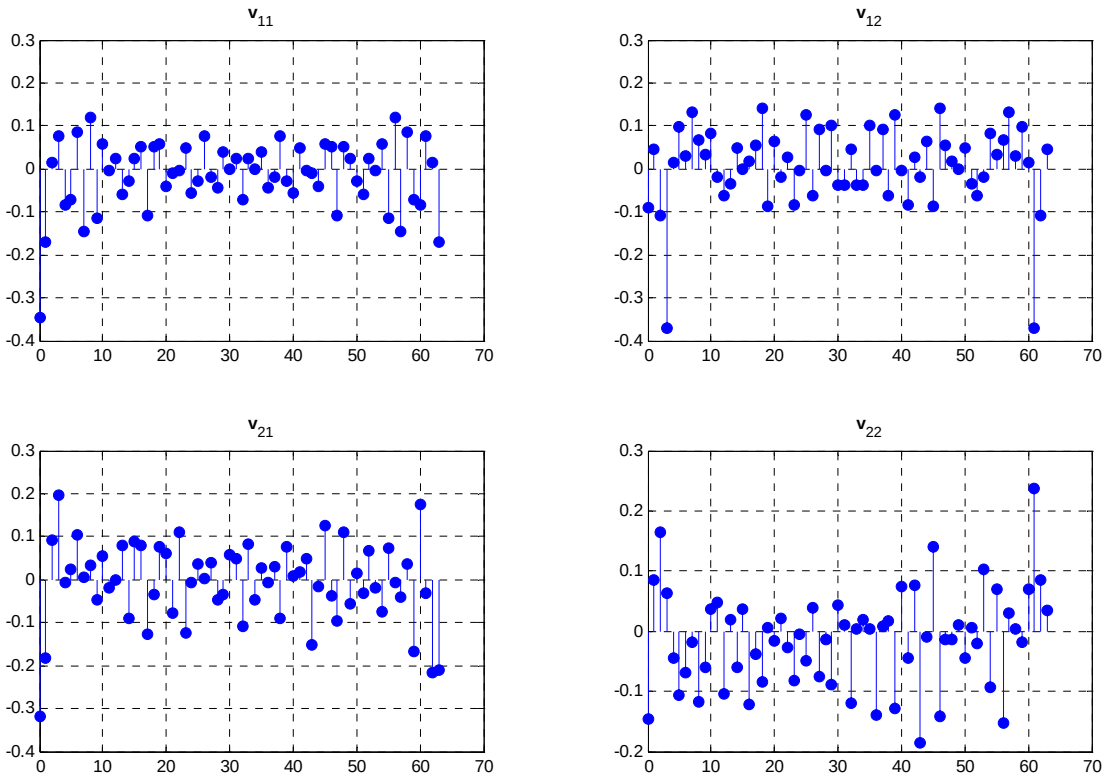

Figure 4.4: *Impulse response of the MIMO Tx filters (64 taps).*

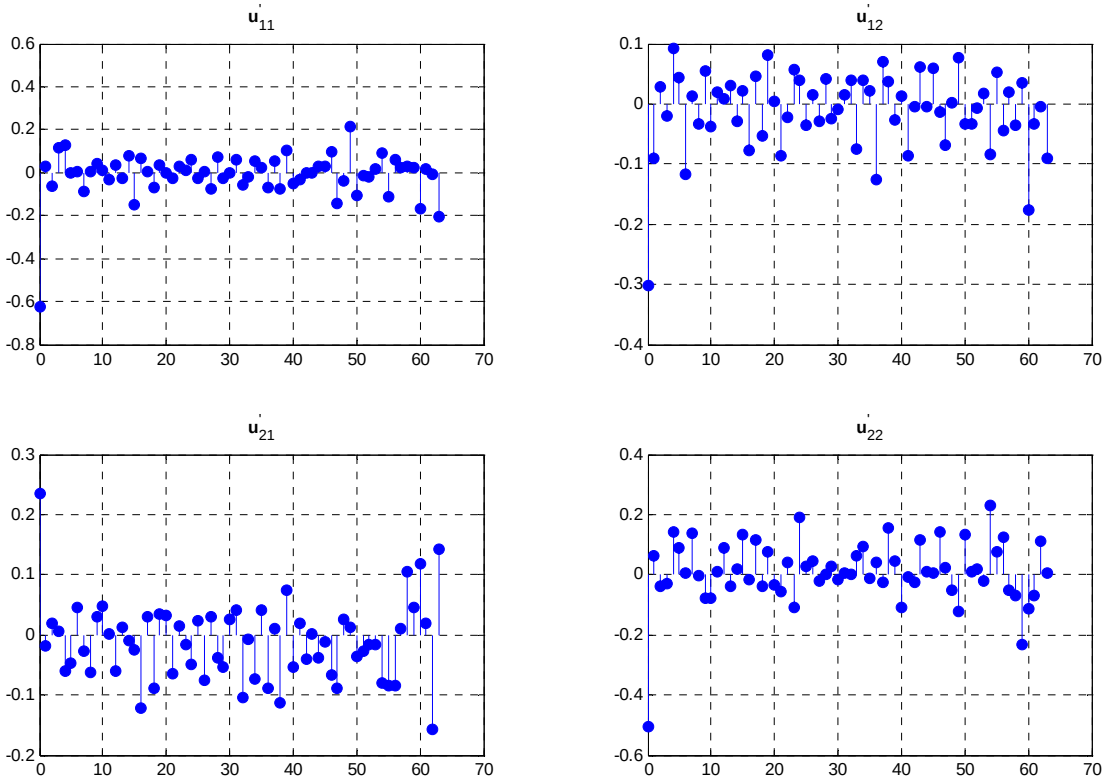

Figure 4.5: *Impulse response of the MIMO Rx filters (64 taps).*

4.2 Water-filling and Adaptive Modulation

When the CSI is known at the transmitter, water-filling can be used to maximize system capacity. Water-filling algorithms work by increasing the transmit power when the SNR at the receiver is high and decreasing the transmit power when SNR is low [14]. Variations in SNR at the receiver will be significant in case of heavy fading. In addition, adaptive modulation can be used for different subchannels i.e. higher level modulation can be used for subchannels with large singular values to increase capacity [4].

For the acoustic MIMO system presented in this thesis, water-filling has not been used because the received signal power at both microphones was reasonably high in absence of external noise sources. Since maximum Tx signal power was used on both channels, further increase in Tx power was not possible. Adaptive modulation could also not be used since higher level modulation techniques do not work well with the acoustic system.

4.3 The Algorithm

Step 1: Take p-point DFT of each subchannel in the channel matrix $\mathbf{H}$ to obtain the matrix $\mathbf{H}_w$.

Step 2: Create subchannel matrices and perform the SVD.

for $k \in \{0, 1, \ldots, p-1\}$

$$\mathbf{H}_w^{(k)} = \begin{bmatrix} h_{w11}(k) & h_{w12}(k) \\ h_{w21}(k) & h_{w22}(k) \end{bmatrix}$$

$$\left[\mathbf{U}_w^{(k)}, \mathbf{D}_w^{(k)}, \mathbf{V}_w^{(k)}\right] = \mathrm{SVD}\left(\mathbf{H}_w^{(k)}\right)$$

$$\mathbf{V}_w(:, k) = \mathbf{V}_w^{(k)}(:, 1)$$

$$\mathbf{V}_w(:, p+k) = \mathbf{V}_w^{(k)}(:, 2)$$

$$\mathbf{U}_w^H(:, k) = \mathbf{U}_w^{(k)H}(:, 1)$$

$$\mathbf{U}_w^H(:, p+k) = \mathbf{U}_w^{(k)H}(:, 2)$$

end

Step 3: Create the MIMO filters $\mathbf{V}$ and $\mathbf{U}^H$ by taking the inverse DFT of each subchannel in $\mathbf{V}_w$ and $\mathbf{U}_w^H$ respectively.

4.4 Results

The BER performance of the MIMO system is presented in this section since it is vital to increasing the overall system capacity. The BER vs. SNR curves have been plotted by adding simulated white Gaussian noise to the actual measured data. The actual BER calculation is based on simultaneous transmission of 30,000 bits from each speaker, utilizing a single set of MIMO Tx and Rx filters throughout the transmission. The curves tend to become flat after around 7.5dB since the BER becomes almost equal to the measured BER. The measured BER corresponds to the highest possible Tx signal power and therefore, to the maximum SNR at the receiver, for this particular environment.

The BER curves show the BER of the received signals (referred to as channel 1 and channel 2 in the figures) with and without MIMO equalization for MIMO subchannel filters of different lengths. Results obtained with bandpass prefiltering are also quite good because of the narrowband Tx signals. Figure 4.6 also shows the BER performance of the MIMO system when channel coding is applied to both independent bit streams using (7,4) Hamming codes. The results are based on transmission of 30,002 bits of encoded data which corresponds to an effective data rate of 17,144 bits without coding.

Use of (7,4) Hamming codes reduces the effective data rate of the MIMO system due to the large overhead. This problem can be addressed by using more efficient coding techniques, like the highly efficient turbo codes [15].

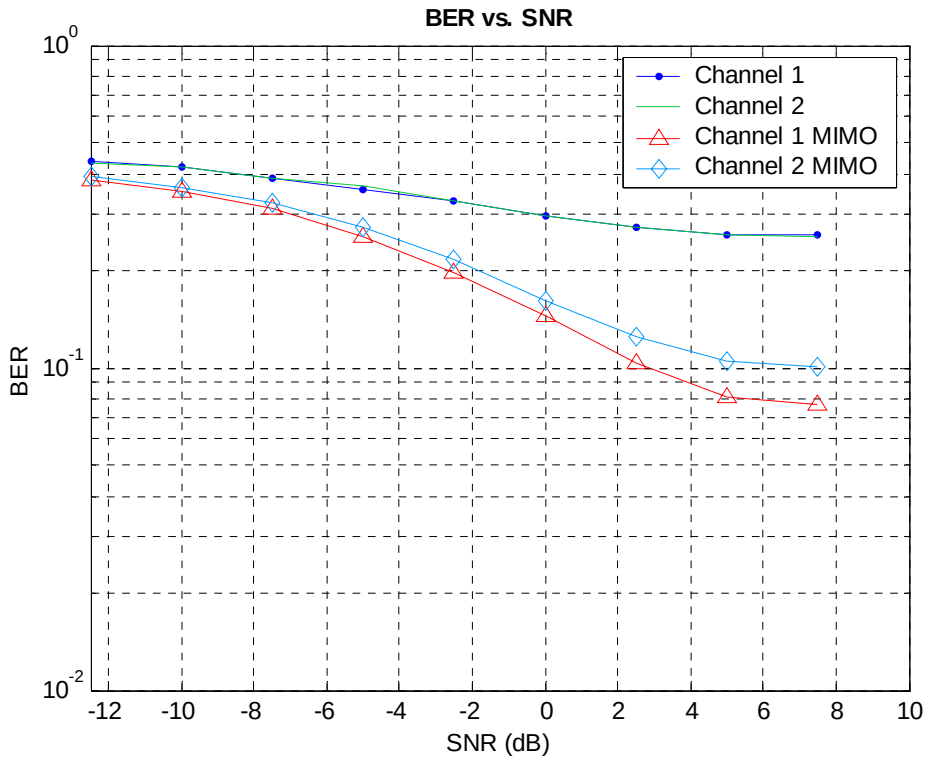

Figure 4.6: *BER vs. SNR curves with 64-tap subchannel filters and highpass prefiltering.*

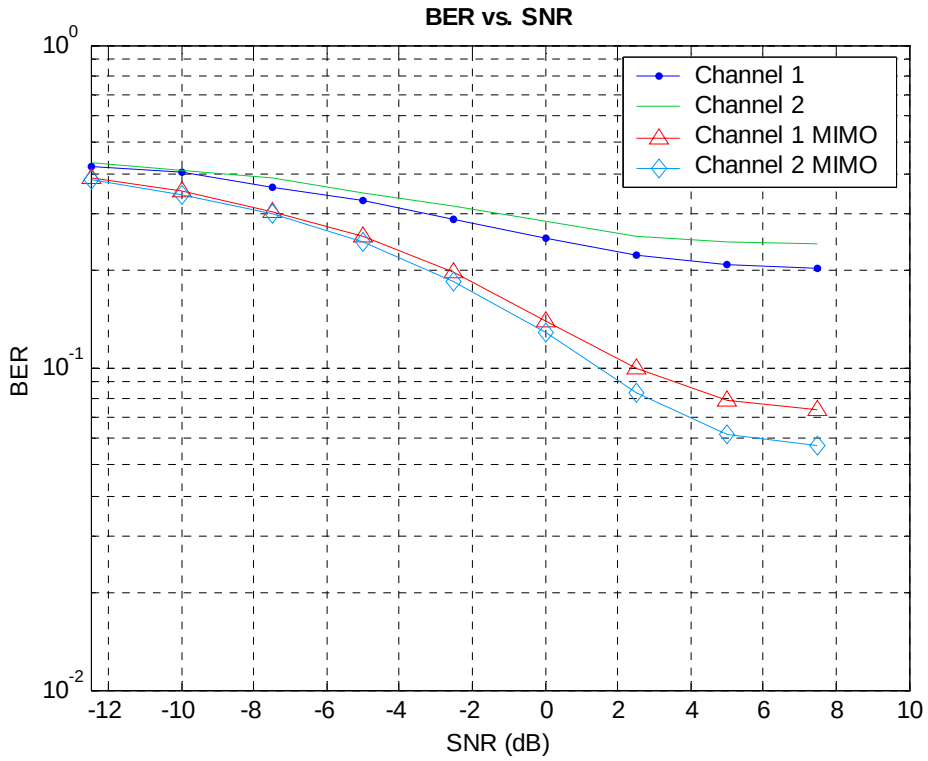

Figure 4.7: *BER vs. SNR curves with 32-tap subchannel filters and highpass prefiltering.*

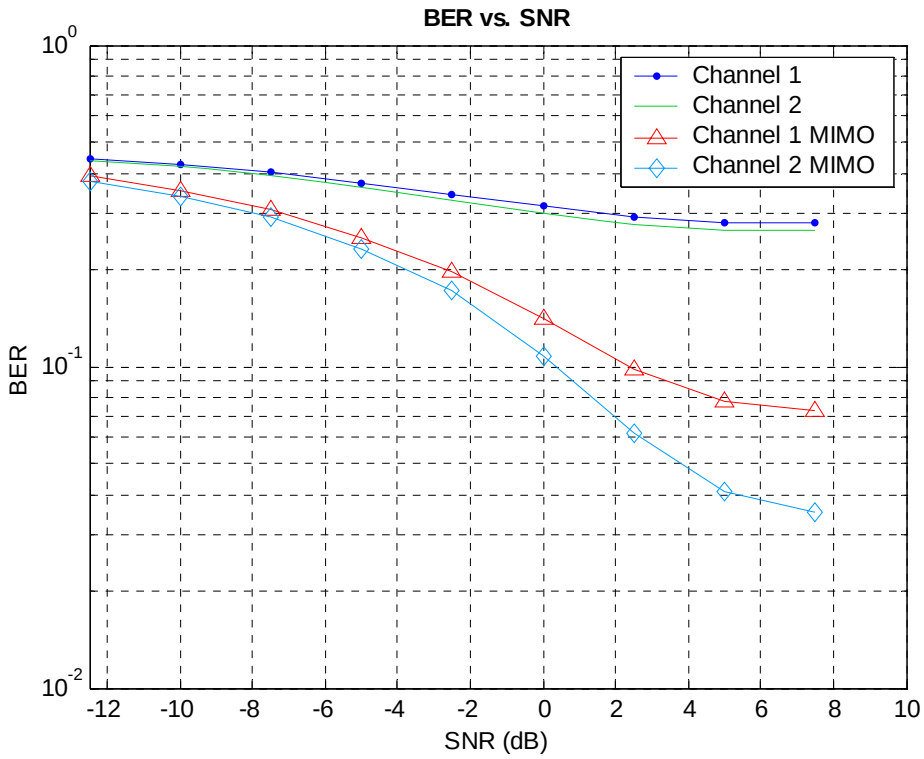

Figure 4.8: *BER vs. SNR curves with 24-tap subchannel filters and highpass prefiltering.*

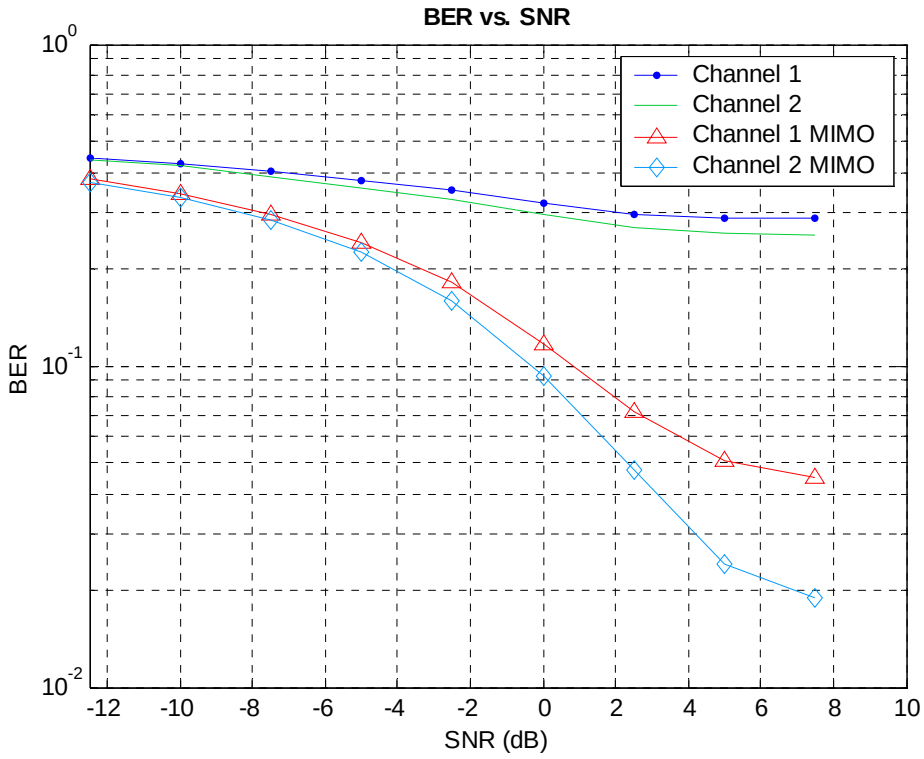

Figure 4.9: *BER vs. SNR curves with 24-tap subchannel filters and bandpass prefiltering.*

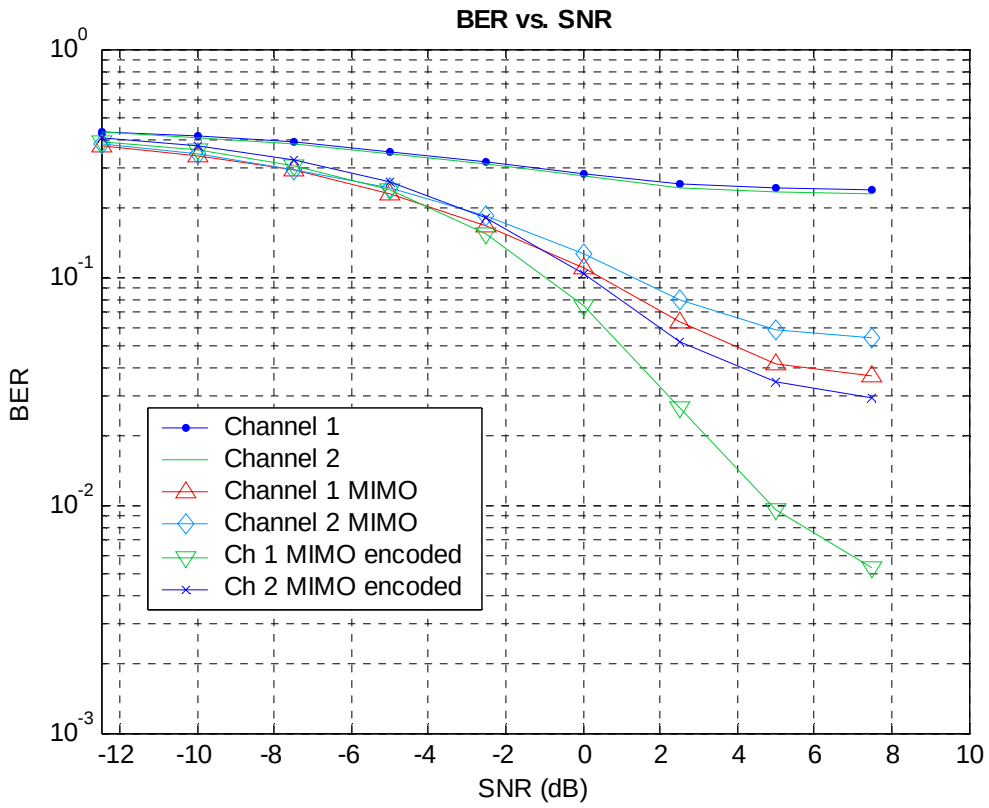

Figure 4.10: *BER vs. SNR curves with 32-tap subchannel filters and highpass prefiltering. Results with channel coding using (7,4) Hamming codes are also shown.*

Conclusions

The acoustic MIMO system presented in this thesis performs reasonably well for sufficient number of filter taps in the estimated subchannels, as seen from the results given in Chapter 4. However, the performance degrades in case of very long subchannel filters, for the reasons explained in section 3.4. Similarly, the performance is severely degraded if very few filter taps are used since the acoustic channel cannot be accurately estimated in this case. This is typically the case with 12 taps or less.

Acoustic channels are generally difficult to estimate and require a large number of filter taps for accurate representation. However, the MIMO system works well with considerably short filter lengths since the relevant channel bandwidth is quite small due to the low transmission data rate.

The performance of the MIMO system can be improved further by using efficient channel coding techniques. In addition, the MIMO algorithm employed in this thesis can be optimized for better results. Further optimization of the channel estimation method may also be possible.

The room where the experiments were conducted contained several objects apart from the reflectors used to create the multipath environment, thus making it difficult to estimate the scattering patterns. A more controlled environment would have resulted in more consistent system performance with smaller variation in the results.

The audio equipment used to create the MIMO system also had certain limitations which affected the capabilities of the system and contributed to errors in implementation. For example, the signal power and bit rate of the transmitted signals could not be increased much and prefiltering of the received signals had to be carried out due to the presence of undesirable components in the microphone frequency response.

References

[1] David Gesbert, Mansoor Shafi, Da-shan Shiu, Peter J. Smith, and Ayman Naguib, "From theory to practice: an overview of MIMO space-time coded wireless systems," *IEEE Journal on Selected Areas in Communications*, vol. 21, no. 3, pp. 281-302, Apr. 2003.

[2] G. D. Golden, G. J. Foschini, R. A. Velenzuela, and P. W. Wolniansky, "Detection algorithm and initial laboratory results using V-BLAST space-time communication architecture," *Electronics Letters*, vol. 35, no. 1, pp. 14-15, Jan. 1999.

[3] S. Sandhu, R. Heath, and A. Paulraj, "Space-time block codes versus space-time trellis codes," in *Proc. IEEE International Conference on Communications*, vol. 4, 2001, pp. 1132-1136.

[4] Yi Jiang, Jian Li, and William W. Hager, "MIMO transceiver design using geometric mean decomposition," in *Proc. IEEE Information Theory Workshop*, Oct. 2004, pp. 193-197.

[5] Michael Zatman and Brian Tracey, "Underwater acoustic MIMO channel capacity," in *Proc. Thirty-Sixth Asilomar Conference on Signals, Systems and Computers*, vol. 2, Nov. 2002, pp. 1364-1368.

[6] Marin Stoytchev and Hugo Safar, "Statistics of the MIMO radio channel in indoor environments," in *Proc. IEEE Vehicular Technology Conference*, vol. 3, Oct. 2001, pp.1804-1808.

[7] M-Audio Delta 1010 website, http://www.m-audio.com/products/en_us/Delta1010-focus.html

[8] Mattias Claesson, "Development of a real-time signal processing framework," M.S. thesis, Dept. Signal Processing, Blekinge Institute of Technology, Ronneby, Sweden, May 2004.

[9] "Anti-causal, zero-phase filter implementation," Signal Processing Toolbox help, Matlab ver. 6.1.0.450 release 12.1, May 2001.

[10] Monson H. Hayes, *Statistical Digital Signal Processing and Modeling*, John Wiley & Sons, 1996.

[11] William Stallings, *Wireless Communications and Networks*, Prentice Hall, 2002.

[12] Simon Haykin, *Digital Communications*, John Wiley & Sons, 1998.

[13] Theodore S. Rappaport, *Wireless Communications: Principles and Practice*, 2nd edition, Prentice Hall, 2002.

[14] Syed Aon Mujtaba, "MIMO signal processing – the next frontier for capacity enhancement", in *Proc. IEEE Custom Integrated Circuits Conference*, Sept. 2003, pp. 263-270.

[15] Farid Dowla, *Handbook of RF and Wireless Technologies*, Elsevier, 2004.